Original article

MOLECULAR METABOLISM

Activation of NF-κB drives the enhanced survival of adipose tissue macrophages in an obesogenic environment

Andrea A. Hill [1,5], Emily K. Anderson-Baucum [1,4,5], Arion J. Kennedy [1], Corey D. Webb [1], Fiona E. Yull [3], Alyssa H. Hasty [1,2,*]

ABSTRACT

Objective: Macrophage accumulation in adipose tissue (AT) during obesity contributes to inflammation and insulin resistance. Recruitment of monocytes to obese AT has been the most studied mechanism explaining this accumulation. However, recent evidence suggests that recruitment-independent mechanisms may also regulate pro-inflammatory AT macrophage (ATM) numbers. The role of increased ATM survival during obesity has yet to be explored.

Results: We demonstrate that activation of apoptotic pathways is significantly reduced in ATMs from diet-induced and genetically obese mice. Concurrently, pro-survival Bcl-2 family member protein levels and localization to the mitochondria is elevated in ATMs from obese mice. This increased pro-survival signaling was associated with elevated activation of the transcription factor, NF-κB, and increased expression of its pro-survival target genes. Finally, an obesogenic milieu increased ATM viability only when NF-κB signaling pathways were functional.

Conclusions: Our data demonstrate that obesity promotes survival of inflammatory ATMs, possibly through an NF-κB-regulated mechanism.

Keywords Adipose tissue; Macrophage; Apoptosis; Cleaved caspase-3; NF-κB; Survival

1. INTRODUCTION

In 2003, two seminal papers demonstrated that macrophages accumulate in adipose tissue (AT) during obesity [1,2]. AT macrophage (ATM) number positively correlates with adiposity, systemic inflammation, and insulin resistance (IR), suggesting that these immune cells play an essential role in the pathogenesis of obesity. Recent findings also demonstrate a role for other immune cell subsets, including T cells [3–6], B cells [7], eosinophils [8], and neutrophils [9], in the control of AT inflammation. However, in mice, macrophages are the most prevalent immune cell type in AT and are a major source of inflammatory cytokines and chemokines secreted from AT during obesity [1,2]. This heightened immune response changes the types and amounts of lipids and adipokines released from AT, which can then negatively impact other tissues and promote metabolic disease [10]. In fact, increased AT inflammation is now considered one of the primary drivers of IR associated with obesity (reviewed in [11]). Thus, the immune system is now at the forefront of metabolic research, and extensive efforts have focused on determining mechanisms by which macrophages accumulate in obese AT.

Obesity increases expression of numerous chemokines and chemokine receptors in AT [12]. Furthermore, labeling studies have shown that obesity results in recruitment of monocytes from the bone marrow into AT [1,13]. Therefore, to date, the majority of published studies have sought to determine whether reducing the chemoattractant potential of AT can inhibit ATM accumulation during obesity. However, in many instances, obese mice genetically lacking certain chemokines or chemokine receptors exhibit no change in ATM number and no improvement in metabolic abnormalities [14–18]. Additionally, even in studies showing that deficiency or antagonism of chemokines decreases ATM number during obesity, macrophage accumulation during high fat diet (HFD) feeding is never completely abolished [13,19–23]. Furthermore, several models with deficiencies in chemoattractant molecules demonstrate a pronounced decrease in circulating inflammatory monocytes without a corresponding large reduction in ATM number [21,24]. Together these findings suggest that recruitment-independent mechanisms may also contribute to the accumulation of pro-inflammatory macrophages in obese AT. Indeed, recently published studies have highlighted that alterations in macrophage proliferation [25,26] and egress [27] contribute to the increased number of ATMs in obesity. In addition to macrophage recruitment, proliferation, and

[1]Department of Molecular Physiology and Biophysics, Vanderbilt University School of Medicine, United States [2]Department of Veterans Affairs, Tennessee Valley Healthcare System, United States [3]Department of Cancer Biology, Vanderbilt University School of Medicine, United States

[4] Department of Medicine, Indiana University School of Medicine, United States.
[5] Andrea A. Hill and Emily K. Anderson-Baucum contributed equally to this work.

*Corresponding author. Vanderbilt University School of Medicine, Room 702 Light Hall, Nashville, TN 37232-0615, United States. Tel.: +1 615 322 5177. E-mail: alyssa.hasty@vanderbilt.edu (A.H. Hasty).

Received June 23, 2015 • Revision received July 10, 2015 • Accepted July 18, 2015 • Available online 28 July 2015

http://dx.doi.org/10.1016/j.molmet.2015.07.005

egress, modification of cell survival/death pathways is another mechanism by which tissue cell number could be modulated.

Regulation of cell survival through the proper control of programmed cell death (apoptosis) is essential for homeostatic maintenance of cell number in many tissues (reviewed in [28]). For example, accelerated apoptosis is observed in neurodegenerative disorders, while impaired apoptosis can contribute to tumorigenesis, autoimmunity, and inflammatory disorders (reviewed in [29]). Interestingly, it is not known whether macrophage apoptosis/survival is modulated in AT during obesity.

The control of cell survival is intricately balanced by the activation of pro-apoptotic and pro-survival signaling pathways. Apoptosis is initiated by either intrinsic or extrinsic pathways, both of which proximally activate the caspase cascade (reviewed in [29]). To oppose apoptosis, cells can activate pro-survival pathways. Much of the balance between cell death and survival is controlled via transcriptional and post-transcriptional regulation of vital factors that maintain mitochondrial outer membrane integrity [30]. The transcription factor, NF-κB, is a key regulator of pro-survival factors such as the Bcl-2 family and inhibitors of apoptosis proteins (IAPs). These proteins are important in preventing caspase-induced cell death, thus allowing for increased survival in many cell types. NF-κB-induced progression of multiple diseases through promotion of cell survival has been well documented [31,32]. Of relevance, a previous study has demonstrated increased nuclear translocation of the p65 subunit of NF-κB in ATMs of obese compared to lean mice [33].

Our findings presented below demonstrate that activation of NF-κB in ATMs during obesity promotes cell survival. Therefore, NF-κB-dependent modulation of the balance between cell survival and death may be an additional mechanism — along with recruitment, proliferation, and retention — that promotes macrophage accumulation in AT during obesity.

2. MATERIALS AND METHODS

2.1. Animal usage and phenotyping

All animal procedures were performed with prior approval from the Institutional Animal Care and Usage Committee of Vanderbilt University. Male C57Bl/6 mice were purchased from Jackson Laboratories. At 8-weeks of age, mice were placed on diets containing either 10% (low fat diet, LFD; Research Diets #D12450B) or 60% (high fat diet, HFD; Research Diets #D12492) of kcal from fat. The diets were protein and micronutrient-matched, providing equivalent quantities of vitamins and minerals. Ob/ob mice (stock number 000632) and lean littermate controls were purchased from Jackson Laboratories at 7 weeks of age and maintained on standard chow diet (LabDiet 5001) until 9—10 weeks of age. NF-κB-GFP-Luciferase (NGL) mice ubiquitously express an enhanced GFP (EGFP)/luciferase gene that is controlled by an enhanced promoter containing two NF-κB binding sites [34]. All mice were given free access to food and water. When indicated, total fat and lean mass were quantified by nuclear magnetic resonance using a Bruker Minispec instrument (Woodlands, TX) in the Vanderbilt Mouse Metabolic Phenotyping Center. Mice were fasted for 5 h before tail vein collection of blood for the determination of glucose levels using a LifeScan One Touch Ultra glucometer (Johnson & Johnson, Northridge, CA).

2.2. Tissue cell isolations

2.2.1. Isolation of AT stromal vascular fraction (SVF)

Mice were euthanized and perfused through the left ventricle with 20 mL of PBS. Epididymal AT was removed and 0.25—0.5 g of tissue was minced in 3 mL PBS with 0.5% FBS. Subsequently, 3 mL of 2 mg/mL collagenase II (Sigma—Aldrich, St. Louis, MO) was added to achieve a final concentration of 1 mg/mL. Tissue was incubated at 37 °C for 20—30 min while shaking at 200 RPM. The cell suspension was then filtered through a 100 μM cell strainer. Cells were spun at 500 × g for 10 min to separate adipocytes from the SVF. The SVF was re-suspended in 3 mL ACK buffer to lyse red blood cells. Cells were washed 2× with PBS, then lysed for Western blot or real-time RT-PCR analysis, or counted using a Cellometer Auto T4 and plated to select for macrophages based upon their strong adhesive properties (see Section 2.2.3 below).

2.2.2. Isolation of hepatocyte and F4/80-enriched fractions from the liver

Mice were euthanized and perfused as described above. The liver was removed and minced in 3 mL RPMI with 5% FBS. Next, 3 mL of 2 mg/mL collagenase II was added and tissue was incubated at 37 °C for 30 min while shaking at 200 RPM. The cell suspension was filtered through a 100 μM cell strainer and spun at 300 RPM for 3 min. The hepatocyte fraction (pellet) was collected for Western blot analysis, while the supernatant (non-parenchymal fraction) was spun at 1500 RPM for 10 min. Cells were then re-suspended in a 33% normo-osmotic Percol solution containing 10 U/mL heparin and spun at 500 × g for 15 min. Subsequently, cells were washed and incubated with Fc block for 10 min and then stained with anti-mouse F4/80-APC (eBioscience, San Diego, CA) at a concentration of 5×10^6 cells/mL. Cells were incubated with anti-APC magnetic beads for 15 min at 4 °C, washed, re-suspended in FACS buffer, and sorted using a Miltenyi AutoMACs magnetic cell sorter. The F4/80-enriched fraction was collected for Western blot analysis.

2.2.3. ATM selection by adherence

Isolated SVF cells (Section 2.2.1) were plated in DMEM with 5% FBS for 2 h in tissue culture dishes with well sizes specific to the subsequent application purpose. The plate was then washed 2× with PBS, leaving any adherent ATMs attached and eliminating all other cells. Attached cells were verified as macrophages based upon positive immunostaining for F4/80 (86.88% ± 0.77% from LFD mice and 87.74% ± 0.72% from HFD mice, quantified from 10 images/group). ATMs were used for the following assays: 1) fixed for immunofluorescence staining (Figures, 5—7), 2) Real-time RT-PCR (Figures 6 & 7), or 3) metabolic cocktail studies (Figure 7).

2.3. Western blot analysis

SVF cells and the F4/80-enriched fraction isolated from the liver were collected in lysis buffer containing 20 mM Tris-HCL (pH 8.0), 150 nM NaCl, 1 mM EDTA, 1 mM EGTA, 0.1% Nonidet P-40, 2.5 mM sodium pyrophosphate, 1 mM sodium orthovanadate, and 0.5 mM PMSF. A modified Lowry protocol was used to quantify protein concentration. Whole AT, hepatocytes, and spleen were sonicated in 500—700 μL of 2% SDS containing 2.5 mM sodium pyrophosphate and 0.5 mM PMSF. Protein was quantified using a bicinchoninic acid (BCA) assay (Thermo Scientific, Waltham, MA). Subsequently, 10—15 μg of protein was electrophoresed through 4—12% Bis-Tris gels (Invitrogen, Grand Island, NY), transferred to a nitrocellulose membrane, and immunoblotted with the following antibodies: cleaved caspase-3, Bax, Bak, Bcl-2, Bcl-xl and phospho-p65. All antibodies were obtained from Cell Signaling Technology (Boston, MA). Blots were developed using either Western Lightning enhanced chemiluminescence substrate and film (Perkin Elmer, Waltham, MA) followed by band intensity quantification using ImageJ64 software, or were imaged using Odyssey

Blocking Buffer and the Li-Cor Odyssey Infrared Imaging System (Li-Cor, Lincoln, NE) followed by band intensity quantification using Image Studio Lite Version 3.1 software.

2.4. Gene expression by real-time RT-PCR

SVF cells were collected in TRIzol reagent (Invitrogen). Total RNA was isolated using a phenol-chloroform extraction, according to the manufacturer's instructions. An iScript cDNA synthesis kit (BioRad, Hercules, CA) was used for reverse transcriptase reactions. Real-time RT-PCR analysis was performed using an iQ5 multicolor real-time PCR detection system (Bio-Rad). Primer-probe sets (Assays-on-Demand) were purchased from Applied Biosystems (Foster City, CA). All genes were analyzed using the Pfaffl method [35] and normalized to *Rplp0*. The expression of the following genes was assessed: *Emr1* (Mm00802530_m1), *Rplp0* (Mm00725448_s1), *Bax* (Mm00432-051_m1), *Bak1* (Mm00432045_m1), *Bcl2* (Mm00477631_m1), *Bcl2l1* (Mm00437783_m1), *Tnf* (Mm00443258_m1), *Xiap* (Mm01 311594_mH), *Birc3* (Mm01168413_m1), *Abca1* (Mm00442646_m1), and *Plin2* (Mm00475794_m1).

2.5. Immunofluorescence microscopy and analysis

2.5.1. Confocal staining of whole AT for TUNEL$^+$ macrophages

PBS perfused epididymal AT was harvested and immediately fixed in 1% paraformaldehyde for 1 h. Tissue was blocked in 5% goat serum in PBS for 1 h and stained with a rat anti-mouse F4/80 antibody (Abcam, Cambridge, MA) overnight at 4 °C. After washing with PBS, tissue was incubated with an Alexa 488-conjugated anti-rat secondary antibody (Cell Signaling Technology) for 1 h at RT. TUNEL staining was performed using the In Situ Cell Death Detection Kit (Roche-Applied Science, Indianapolis, IN), according to manufacturer's instructions. Tissue was then counter-stained with DAPI (0.2 mg/mL) and imaged at 40× magnification using an Olympus FV-1000 Inverted Confocal Microscope. In order to avoid endogenous tissue autofluorescence, tissues were first imaged under the DAPI filter. Areas with no autofluorescence were then selected for imaging. There was no apparent pattern to which areas of AT displayed autofluorescence. CLSs were determined by eye as a small adipocyte surrounded by macrophages as reported by other groups [36–38]. All other macrophages were considered interstitially spaced macrophages. At least 3 images were captured from 4 to 7 mice per group.

2.5.2. Automated and confocal imaging for nuclear and mitochondrial co-localization

The Image Xpress Automated Micro XL Microscope with Meta Xpress analysis software in the High-Throughput Screening Core at Vanderbilt University was used for these studies. SVF was collected and ATMs were adherence-selected in a 96-well plate, as described above. Adherent ATMs were then fixed with 4% PFA for 1 h. ATMs were stained with antibodies against F4/80 and Bax, Bcl-2, or p65 (Cell Signaling Technology) in order to determine co-localization with nuclear (DAPI) and mitochondrial (Cox IV, Abcam, Cambridge, MA) markers. Images were acquired from 4 areas per well at 40× magnification on the Image Xpress Automated Micro XL Microscope. An analysis software module was developed to allow for quantification of the overlap of the fluorescence signal of a specific protein with a defined organelle compartment of interest (nucleus or mitochondria). Analysis parameters were set to identify macrophages (F4/80$^+$) with intact nuclei (DAPI positive, diameter of 2–8 μm) and mitochondria (Cox IV, diameter of 1–3 μm). Co-localization data was collected from 10,000 to 30,000 ATMs per mouse from 6 to 7 mice per group. For statistical purposes, the average co-localization from all the macrophages of an individual mouse was counted as a single biological replicate. To obtain higher quality images for the purpose of visualization and confirmation of these computed changes, the representative images displayed in Figures 5 and 6 were performed using an Olympus FV-1000 Inverted Confocal Microscope at 100× or 60× magnification with a 1.5 or 4.5 zoom. All images were taken at the same magnification, voltage, and gain level required for proper imaging in each channel. To perform these studies, ATMs were plated in 8 well chamber slides for 2 h to allow for selection by macrophage adherence. ATMs were then fixed for 1 h with 4% PFA, and stained for DAPI, p65, Bax and Bcl-2 as described. Mitochondria were stained using MitoTracker Deep Red FM (Life Technologies, Grand Island, NY) at 100 nM for 25 min.

2.6. Ex vivo studies in isolated ATMs

2.6.1. NF-κB-regulated luciferase reporter assay

ATMs were collected from NGL mice by SVF isolation and macrophage selection by adherence, as described above. ATMs were washed once with PBS followed by the addition of 20 μL of luciferase lysis buffer (Promega, Madison, WI). Luciferase substrate was added to the sample and luminescence was immediately read on a Monolight 3010 (BD PharMingen, San Diego, CA).

2.6.2. Metabolic activation of ATMs

ATMs were treated with a metabolic cocktail (MetaC) containing 30 mM glucose, 10 nM insulin and 0.4 mM palmitic acid as previously described [39]. Palmitic acid was dissolved in ethanol and added to DMEM containing 5% FBS, 30 mM glucose and 10 nM insulin. ATMs were treated with the MetaC in the presence or absence of 10 μM BMS-345541 (Sigma–Aldrich) to inhibit NF-κB. ATMs in the BMS treatment groups were pretreated with 20 μM BMS-345541 for 1 h prior to time-course studies. ATMs were exposed to MetaC for a time-course of 0–8 h.

2.6.3. Cell-Titer Blue assay

ATMs were adherence-selected and plated in 96-well plates. Metabolic activation cocktail studies were performed as described in Section 2.6.2. Cell-Titer Blue reagent (Promega) was added at a volume of 20 μL to wells containing 100 μL of media 2 h prior to end of each time-point. Fluorescence was measured at $560_{Ex}/521_{Em}$ using the GloMax Discover System (Promega). Background fluorescence was measured in wells containing media and Cell-Titer Blue only (*i.e.* without cells) and was subtracted from each experimental measurement.

2.7. Statistical analysis

GraphPad Prism 5.0 software was used for all statistical analyses. Data was analyzed using a two-tailed unpaired *t*-test to determine differences between two groups or a one-way ANOVA when more than two treatment groups were compared. Outliers were excluded from the data for each individual parameter using the Grubbs outlier test [40]. A p value of <0.05 was considered significant.

3. RESULTS

3.1. Diet-induced obesity decreases ATM apoptosis

To determine the impact of obesity on ATM apoptosis and survival, mice were fed 10% LFD or 60% HFD for 9 weeks (Figure S1A). As expected, mice fed HFD became obese, gained lean and fat mass, and

were hyperglycemic compared to LFD-fed controls (Figure S1B–E). Additionally, expression of *Emr1* (the gene for F4/80) in the stromal vascular fraction (SVF) of AT was significantly increased by obesity ($p < 0.05$, Figure S1F), confirming that 9 weeks of HFD feeding is sufficient to promote the accumulation of macrophages in AT.

Recent studies suggest that obesity increases apoptosis in whole AT, likely due to adipocyte cell death resulting from local hypoxia and/or decreased vasculature [36,38,41,42]. Consistent with these findings, HFD feeding increased expression of the pro-apoptotic proteins Bax ($p < 0.001$) and Bak ($p < 0.01$) in AT, although it did not affect caspase-3 cleavage (Figure S2). These data support the concept that obesity increases apoptosis in whole AT. However, the metabolic regulation of apoptosis in ATMs during obesity has not been explored. To determine if obesity alters apoptotic signaling in AT immune cells, protein was isolated from the SVF of AT and assessed for apoptotic markers by Western blot analysis. Remarkably, HFD-fed mice demonstrated a 50% decrease in SVF cleaved caspase-3 protein levels compared to LFD-fed controls, suggesting decreased AT immune cell apoptosis during obesity ($p < 0.001$, Figure 1A). Although the SVF is a macrophage-enriched cell preparation, other leukocytes and pre-adipocytes are also contained within this fraction. To determine if obesity decreases apoptosis specifically in macrophages, AT was stained for F4/80, DAPI, and the apoptosis marker TUNEL. In both LFD- and HFD-fed mice, around 10–20% of cells with TUNEL$^+$ nuclei were F4/80 negative, and about 80–90% of the apoptotic cells were macrophages, indicating that macrophages are the major cell type undergoing apoptosis in the AT (data not shown). Interestingly, quantification of confocal images demonstrated that ~17% of all macrophages in lean AT were TUNEL$^+$ (apoptotic), while only ~4% of macrophages in obese AT were TUNEL$^+$ ($p < 0.0001$, Figure 1B–C). This decrease in apoptotic ATMs was also detected when quantified as number per high power field ($p < 0.01$; Figure 1D). As expected, because almost all ATMs in lean AT are interstitially spaced, the apoptotic ATMs in lean mice were also interstitially spaced (Figure 1E). Even in obese AT, about 50% of the apoptotic ATMs were localized to interstitial spaces.

To determine whether the degree of obesity altered ATM apoptosis, we analyzed mice fed HFD for an extended time period of 16 weeks. These mice displayed an even further 75% decrease in cleaved caspase-3 levels in the SVF ($p < 0.0001$), and a decrease in TUNEL positive ATMs ($p < 0.05$) compared to mice on LFD for 16 weeks (Figure 2A–B). Interestingly, when the data from mice fed LFD or HFD for either 9 or 16 weeks were combined (Figure 2C), a clear negative correlation between body weight and the level of cleaved caspase-3 in SVF was found ($r^2 = 0.48$, $p < 0.0001$). Furthermore, even when only HFD-fed mice (9 and 16 weeks HFD) were included in the analysis (Figure 2D), SVF cleaved caspase-3 levels remained negatively correlated with body weight ($r^2 = 0.24$, $p < 0.05$), suggesting that obesity drives the decrease in AT immune cell apoptosis.

3.2. Genetic obesity decreases ATM apoptosis

To determine if the decreased macrophage apoptosis observed in obese AT was the result of dietary intervention or due to overt obesity, we analyzed a mouse model of genetic obesity. Leptin-deficient ob/ob mice and lean littermate controls were maintained on a chow diet until 9–10 weeks of age, at which point they were of similar weight to the mice fed HFD for 9 weeks. As expected, ob/ob mice were obese compared to lean littermate control mice ($p < 0.0001$; Figure S3A) and

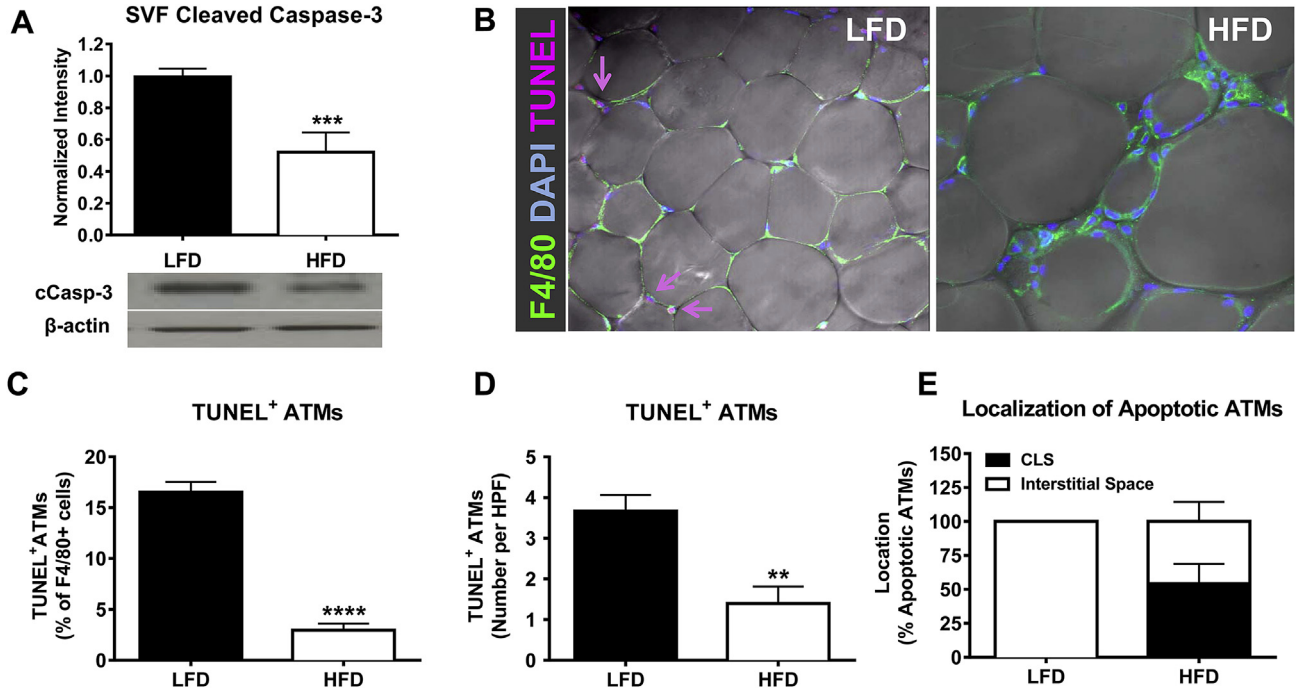

Figure 1: HFD feeding decreases apoptosis of ATMs. Male C57Bl/6 mice were placed on LFD or HFD for 9 weeks. A) SVF was collected and cleaved caspase-3 was analyzed using Western blot. B) AT explants were collected and analyzed by confocal staining for the macrophage marker F4/80 (green), nuclear stain DAPI (blue), and apoptosis marker TUNEL (pink). Magnification: 40×. C–D) Quantification of TUNEL positive ATMs by percent of F4/80 positive cells (C) or by number per high-power field (D). E) Quantification of localization of apoptotic ATMs. Data are presented as mean ± SEM, A) n = 11–14/group, C–D) n = 4–8/group for confocal imaging.**$p < 0.01$, ***$p < 0.001$, ****$p < 0.0001$ between groups.

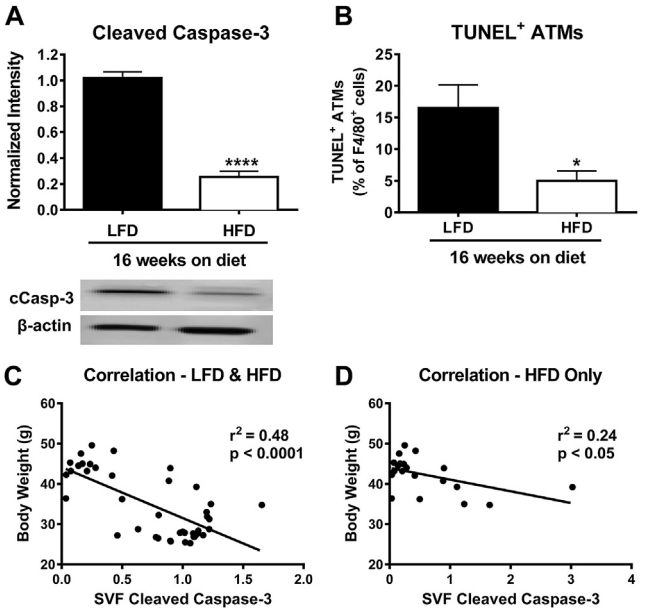

Figure 2: Apoptosis of ATMs is negatively correlated with body weight. Male C57Bl/6 mice were placed on a LFD or HFD for 16 weeks. A) SVF was collected and cleaved caspase-3 was analyzed using Western blot. B) Quantification of TUNEL positive ATMs by percent of F4/80 positive cells. C) Correlation of SVF cleaved caspase-3 with body weight of mice fed LFD and HFD for either 9 or 16 weeks. D) Correlation of SVF cleaved caspase-3 with body weight for HFD fed mice only. A–B) Data are presented as mean ± SEM, n = 5–6/group. *p < 0.05, ****p < 0.0001 between groups.

were hyperglycemic ($p < 0.001$; Figure S3B). Further, the increase in body weight in the ob/ob mice was due to elevated fat mass, rather than lean mass ($p < 0.0001$; Figure S3C–D).

Caspase-3 cleavage was significantly decreased in the SVF of ob/ob mice compared to lean controls ($p < 0.01$, Figure 3A). AT was evaluated by confocal microscopy to determine if genetic obesity decreased apoptosis in macrophages. Quantification of confocal images demonstrated that macrophage apoptosis is significantly decreased in the AT of ob/ob mice compared to lean controls ($p < 0.01$ and $p < 0.05$, Figure 3B–D). Additionally, 50% of apoptotic macrophages were localized to interstitial spaces, rather than crown-like structures (Figure 3E). Thus, both diet-induced and genetic obesity result in decreased ATM apoptosis.

3.3. The obesity-related decrease in macrophage apoptosis is AT-specific

To determine if obesity modulates apoptosis in a similar manner in other metabolically-relevant tissues, protein was isolated from hepatocytes and an F4/80-enriched non-hepatocyte fraction of the liver of mice fed LFD or HFD for 9 weeks. Markers of apoptosis, including protein levels of cleaved caspase-3, Bax, and Bak, were not modified by HFD feeding in either the hepatocyte fraction (Figure S4A–C) or the F4/80-enriched fraction of the liver (Figure S4D–F). Additionally, obesity did not impact markers of apoptosis in the spleen, an immune cell-enriched organ (Figure S4G–I). Therefore, while obesity decreased markers of macrophage apoptosis in AT, apoptosis was not modulated in macrophages of the liver or whole spleen, indicating that this regulation is specific to AT.

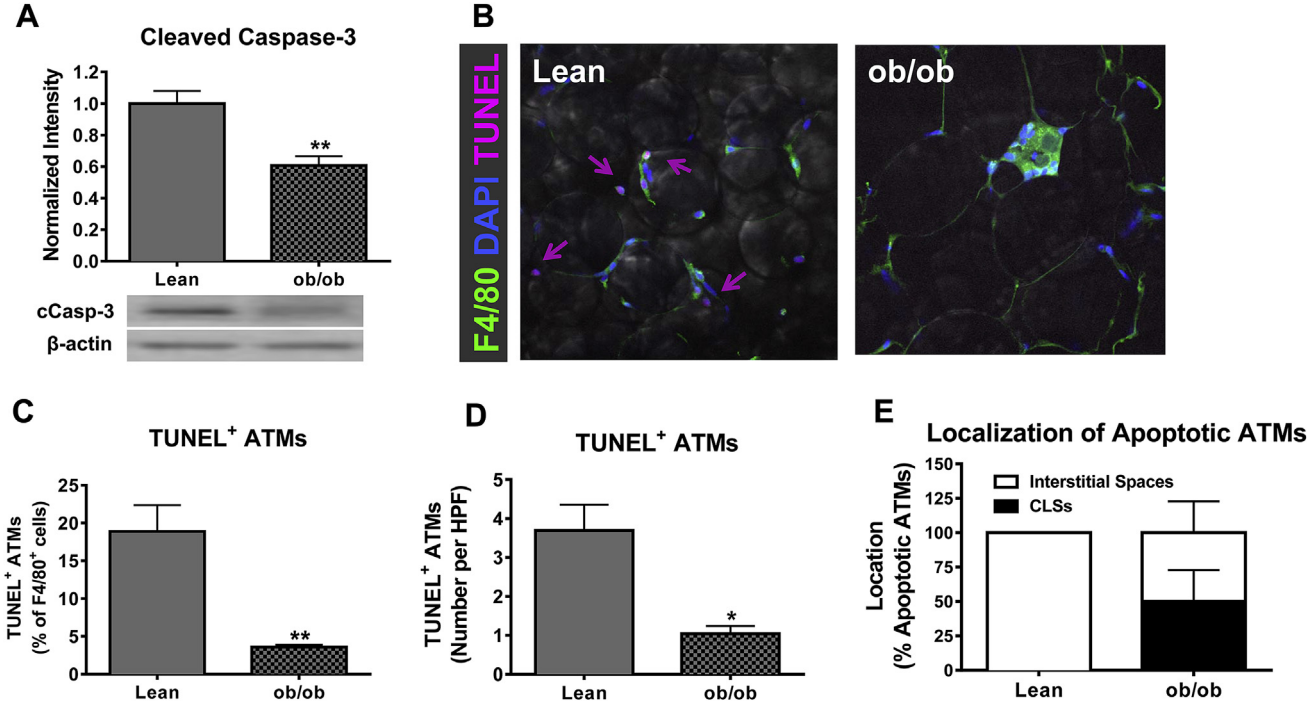

Figure 3: Genetic model of obesity decreases apoptosis of ATMs. Male C57Bl/6 lean or ob/ob mice were maintained on chow diet until 9–10 weeks of age. A) SVF was collected and cleaved caspase-3 was analyzed using Western blot. B) AT explants were collected and analyzed by confocal staining for the macrophage marker F4/80 (green), nuclear stain DAPI (blue), and apoptosis marker TUNEL (pink). Magnification: 40×. C–D) Quantification of TUNEL positive ATMs by percent of F4/80 positive cells (C) or by number per high-power field (D). E) Quantification of localization of apoptotic ATMs. Data are presented as mean ± SEM, A) n = 5/group, C–E) n = 4–6/group. *p < 0.05, **p < 0.01 between groups.

3.4. Decreased markers of ATM apoptosis correlate with increased protein levels of total and mitochondrial-localized pro-survival Bcl-2 protein

A common intrinsic mechanism to regulate apoptosis is maintenance of the integrity of the mitochondrial outer membrane. Within the Bcl-2 family, Bax and Bak are pro-apoptotic, promote mitochondrial outer membrane permeabilization (MOMP), and activate the caspase cascade. Conversely, Bcl-2 and Bcl-xl are pro-survival and inhibit the pore-forming activities of Bax and Bak (reviewed in [43]). To determine if obesity increases immune cell survival through the modulation of Bcl-2 family members, RNA and protein were isolated from the SVF of mice placed on LFD or HFD for 9 weeks. SVF from obese mice displayed increased gene expression of *Bax* ($p < 0.01$, Figure 4A), with no change in the gene expression of other Bcl-2 family members (*Bak1, Bcl2, Bcl2l1* (gene for Bcl-xl), Figure 4B-D). At the protein level, there was a significant increase in Bax ($p < 0.0001$, Figure 4E) in SVF of obese mice, while Bak protein expression was significantly decreased ($p < 0.0001$, Figure 4F). Interestingly, levels of the pro-survival protein, Bcl-2, were 2.5-fold elevated in SVF of obese compared to lean mice ($p < 0.001$, Figure 4G), while no change was seen in Bcl-xl (Figure 4H). These data demonstrate that obesity modifies the protein expression of both pro-apoptotic and pro-survival members of the Bcl-2 family in AT immune cells.

The total protein level of Bcl-2 family members is not the sole determinant of cell survival versus apoptosis. Instead, their localization to the outer membrane of the mitochondria is essential (reviewed in [30,43,44]). To determine if the subcellular localization of the major Bcl-2 family members, Bax (pro-apoptotic) and Bcl-2 (pro-survival) was altered specifically in ATMs during obesity, adherence selected macrophages from the SVF of LFD and HFD mice were assessed. To quantitatively analyze the mitochondrial localization of Bax and Bcl-2, we used automated high-throughput fluorescent microscopy and analysis software described in the Methods section. We first used the Image Xpress imaging technique to quantitatively determine the amounts of Bax and Bcl-2 protein localized to the mitochondria (based upon co-localization with Cox IV) in ATMs of lean and obese mice. Although total protein levels of Bax were increased in the SVF during obesity (Figure 4E), there was no difference in the localization of Bax to the mitochondria in ATMs of LFD versus HFD fed mice (Figure 5A). Interestingly, obesity increased the localization of the pro-survival protein, Bcl-2, to the mitochondria of ATMs ($p < 0.05$, Figure 5B). To confirm the changes quantified using Image Xpress software, we also used confocal microscopy to visualize the differences in Bax and Bcl-2 mitochondrial localization (based upon co-localization with MitoTracker Deep Red). In support of our Image Xpress quantification data, the confocal images show that there was no apparent difference in Bax protein co-localization with mitochondria in ATMs from lean versus obese mice (Figure 5C). However, Bcl-2 protein was highly co-localized to the mitochondria in ATMs of obese compared to lean mice (Figure 5D). Together, the data from Figures 4 and 5 suggest that the increased protein levels and mitochondrial localization of Bcl-2 may allow for increased ATM survival observed during obesity.

3.5. NF-κB activity and its pro-survival gene targets are activated in ATMs of obese mice

A key mediator of inflammatory gene expression in macrophages is the transcription factor NF-κB. A previous study has demonstrated greater localization of the p65 subunit of NF-κB to the nucleus of ATMs during obesity [33]. In addition to its control of inflammatory gene expression, NF-κB also promotes cell survival through the transcription of pro-survival Bcl-2 family members [45]. Therefore, we hypothesized that increased NF-κB activity during obesity might promote ATM survival. To confirm NF-κB activation in ATMs from obese mice, the protein

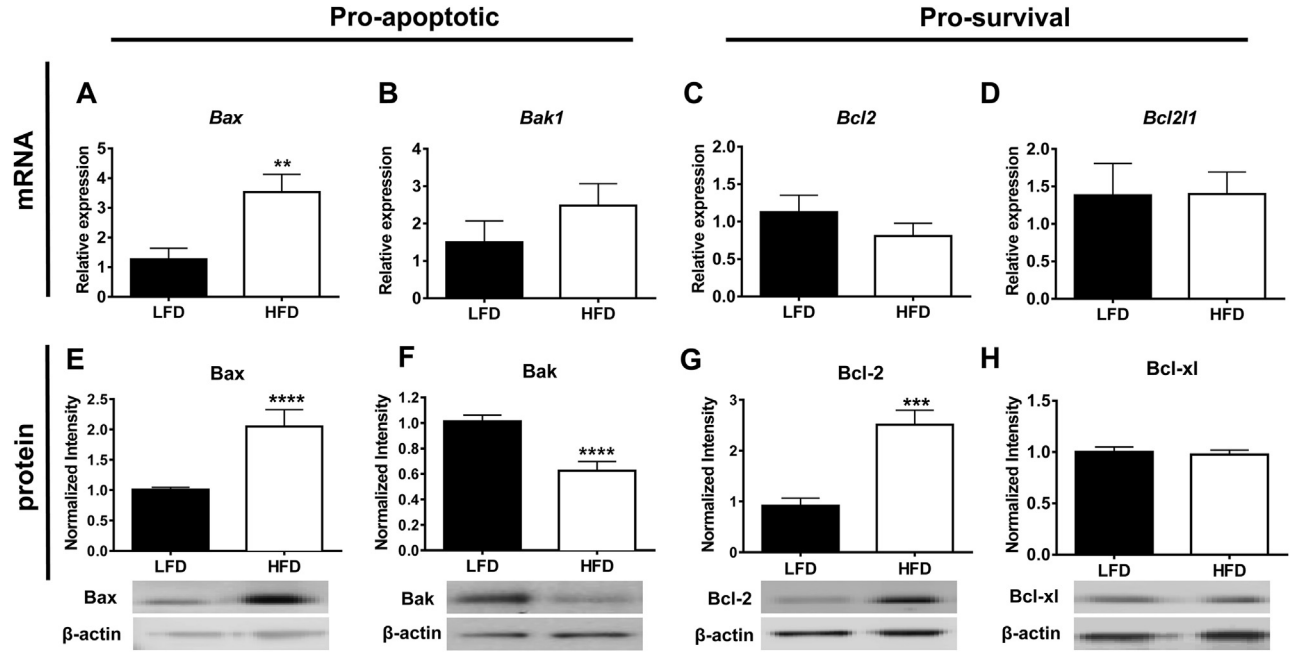

Figure 4: Pro-apoptotic/survival Bcl-2 family members are differentially regulated in the SVF of AT of obese mice. Male C57Bl/6 mice were placed on LFD or HFD for 9 weeks. A–D) SVF was collected and Bcl-2 family pro-apoptotic/survival gene expression was analyzed using real-time RT-PCR: A) *Bax*, B) *Bak1*, C) *Bcl2*, and D) *Bcl2l1*. E–H) SVF was collected and Bcl-2 family pro-apoptotic/survival protein levels were analyzed using Western blot: E) Bax, F) Bak, G) Bcl-2, and H) Bcl-xl. mRNA levels were normalized to housekeeping gene *Rplpo* and levels of specific proteins were normalized to β-actin. Data are presented as mean ± SEM, A-D) n = 7/group, E–F) n = 17–19/group, G-H), n = 4–8/group. **$p < 0.01$, ***$p < 0.001$, ****$p < 0.0001$ between groups.

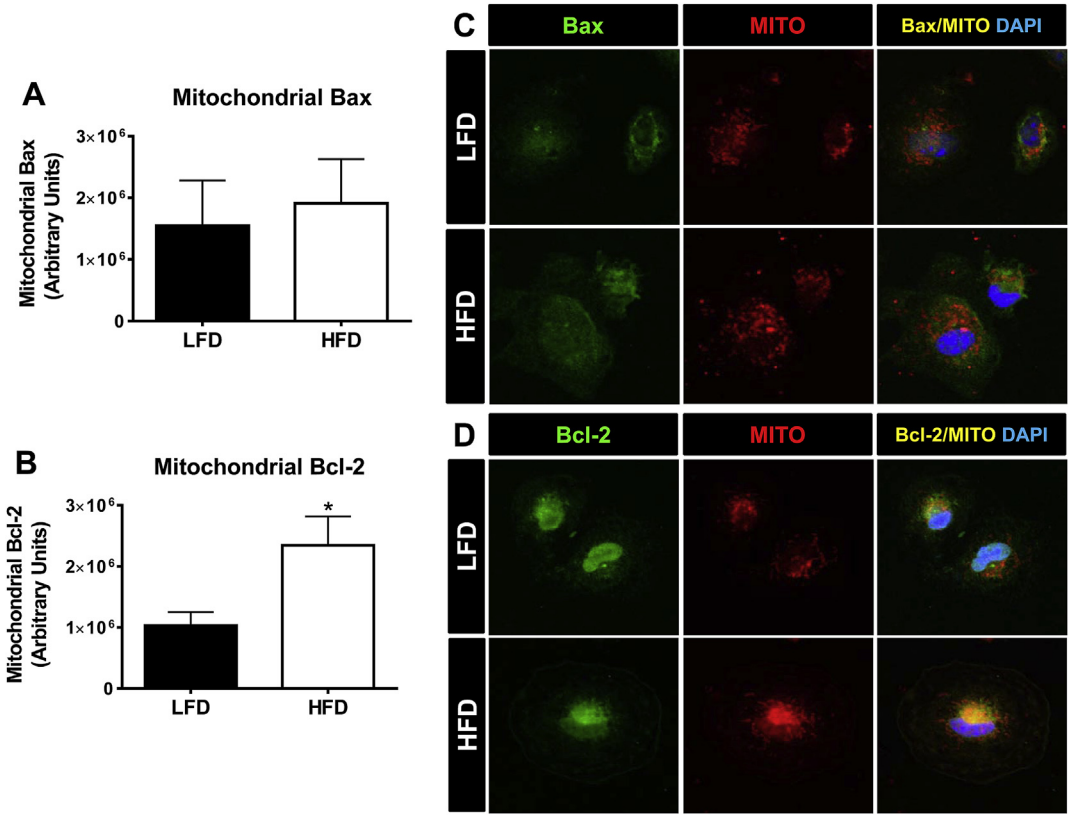

Figure 5: Mitochondrial localization of the pro-survival protein Bcl-2 is increased in ATMs of obese mice. Male C57Bl/6 mice were placed on a LFD or HFD diet for 9 weeks. ATMs were obtained using a 2 h macrophage selection by adhesion assay and stained for quantification of Bax and Bcl-2 mitochondrial localized protein levels using Image Xpress Automated HTS Fluorescence Microscopy or visualization by confocal microscopy. A) Quantification of the co-localization of Bax to the mitochondria of ATMs. B) Quantification of the co-localization of Bcl-2 to the mitochondria of ATMs. Magnification for quantifications: 40×. C) Representative images of Bax (green) mitochondrial (red, MitoTracker (Mito)) localization by confocal microscopy. D) Representative images of Bcl-2 (green) mitochondrial (red, MitoTracker (Mito)) localization by confocal microscopy. Magnification for representative images: 60× with a 4.5 zoom. Data are presented as mean ± SEM, n = 6–7/group. *p < 0.05 between groups.

level of the phosphorylated (active) form of the p65 subunit (P-p65) was assessed in the SVF of mice fed LFD or HFD for 9 weeks. P-p65 was significantly increased in the SVF of HFD mice ($p < 0.05$, Figure 6A). Furthermore, nuclear localization of p65 was increased in adherence-selected ATMs from obese compared to lean mice by confocal microscopy (Figure 6B) and as quantified by Image Xpress Automated HTS Fluorescent Microscopy ($p < 0.001$; HFD: $1.3 \times 10^6 \pm 1.1 \times 10^5$ RLU, and LFD: $0.82 \times 10^6 \pm 0.44 \times 10^5$ RLU, $N = 7$). Next, we determined the transcriptional activity of NF-κB in adherence-selected ATMs through the use of NF-κB promoter-driven GFP-Luciferase reporter mice (NGL) described previously [34]. Luciferase activity was significantly increased in ATMs of obese mice, indicating elevated NF-κB transcriptional activity ($p < 0.05$, Figure 6C). To determine if increased NF-κB transcriptional activity resulted in elevated expression of NF-κB target genes, expression of the inflammatory cytokine, *Tnf*, and the pro-survival inhibitors of apoptosis, *Xiap* and *Birc3* (gene name for cIAP), was analyzed specifically in adherence-selected ATMs. As expected, *Tnf* gene expression was significantly increased in ATMs of HFD-fed mice ($p < 0.05$, Figure 6D). Interestingly, there was a trend towards an increase in *Xiap* expression ($p = 0.07$) and a significant increase in *Birc3* expression ($p < 0.05$) in ATMs from obese mice (Figure 6D). These data demonstrate that increased NF-κB transcriptional activity in ATMs promotes the expression of pro-survival genes. Therefore, it is likely that NF-κB contributes to the increased ATM survival observed during obesity.

3.6. Metabolic activation-induced survival of ATMs is blunted by inhibition of NF-κB

In previous studies, it has been shown that exposing bone marrow-derived macrophages (BMDMs) to high levels of glucose, insulin and palmitate ("metabolic activation") induces a gene expression profile/phenotype similar to ATMs of obese mice [39]. We sought to determine if exposure of ATMs to this metabolic activation cocktail (MetaC; 30 mM glucose, 10 nM insulin and 0.4 mM palmitic acid) would result in increased NF-κB activation, augmented expression of its pro-survival target genes, and increased cell viability. We felt it was important to perform these studies, specifically in ATMs, as recent data from the Immunological Genome Project emphasize the fact that macrophages derived from different tissue/cellular sources have vastly different transcriptomes [46]. Therefore, in order to obtain a sufficient number of ATMs for these studies, mice were fed HFD for 3 weeks prior to the isolation of adherence-selected ATMs. This short-term HFD feeding did not significantly increase NF-κB activity, as measured by NGL luciferase activity (Supplemental Figure 5A). Subsequently, the adherence-selected ATMs were exposed to control or MetaC conditions for 30 min and p65 nuclear localization was visualized using confocal microscopy. In support of our *ex vivo* results, exposure of ATMs to the obesogenic milieu (MetaC) increased nuclear localization of the p65 subunit of NF-κB (Figure 7A). Furthermore, 2 h of metabolic activation of ATMs recapitulated the reported [39] gene expression profile of ATMs *in vivo* (*Tnf*, $p < 0.05$, *Abca1*; $p = 0.09$, *Plin2*;

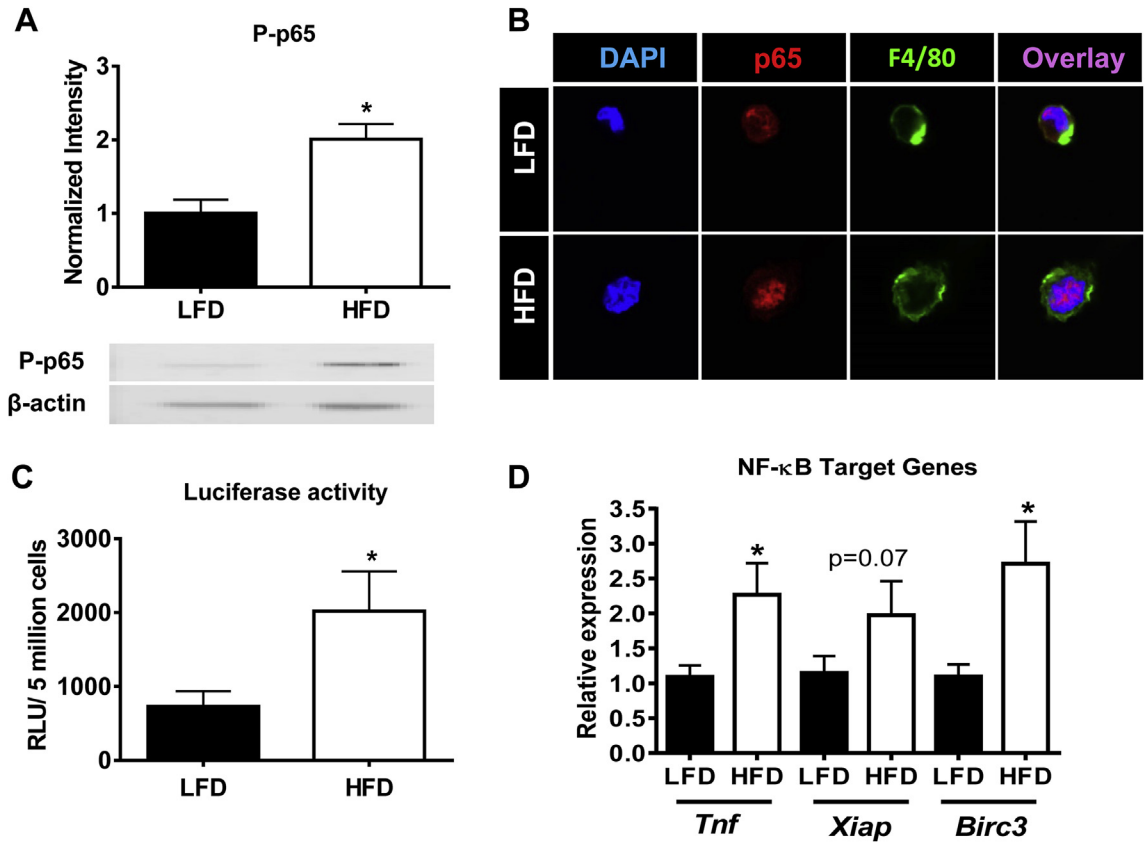

Figure 6: NF-κB activity and its pro-survival target genes are increased in ATMs of obese mice. Male C57Bl/6 mice were placed on a LFD or a HFD for 9 weeks. A) SVF was collected and phosphorylated p65 (P-p65) was analyzed using Western blot. B) Nuclear localization of the p65 subunit of NF-κB. ATMs were obtained using a 2 h macrophage selection by adhesion assay and stained for nuclear stain DAPI (blue), p65 (red), F4/80 (green). Magnification: 100× with a 4.5 zoom. C) Transcriptional activity of NF-κB in ATMs using NF-κB-GFP-Luciferase mice. D) Real-time RT-PCR analysis of NF-κB-driven pro-inflammatory and pro-survival target genes in ATMs (*Tnf, Xiap, Birc3*). Data are presented as mean ± SEM, A) n = 4/group, C) n = 9–10/group, and D) n = 7–8/group. *p < 0.05 between groups.

p = 0.06). Of note, metabolic activation in ATMs also significantly increased the levels of NF-κB pro-survival target genes *Bcl2* (p < 0.05) and *Xiap* (p < 0.05), while modestly increasing *Birc3* (Figure 7B). These findings demonstrate that metabolic activation of ATMs increases NF-κB transcriptional activity and pro-survival gene expression, similar to what we observed *in vivo* during obesity. Interestingly, exposure of ATMs to MetaC alone significantly increased cell viability at 6 and 8 h post-treatment (p < 0.01 and p < 0.05, respectively; Figure 7C), supporting our earlier data demonstrating that the *in vivo* obese milieu promotes ATM survival. We next used this model system to determine the role of NF-κB activation in this increased ATM survival under obesogenic conditions by treating ATMs with MetaC in the presence or absence of the highly selective NF-κB inhibitor, BMS-345541 [47]. Importantly, MetaC increased and BMS inhibited NGL luciferase activity in metabolically activated ATMs from chow-fed mice, indicating that BMS does, in fact, decrease NF-κB activity (Supplemental Figure 5B). In support of our hypothesis, inhibition of NF-κB in ATMs reduced the pro-survival effect of MetaC, a finding that trended at 4 and 8 h of treatment and was significant (p < 0.05) at 6 h of treatment. Taken together, these data suggest that NF-κB activation in ATMs in the obese state increases their ability to survive.

4. DISCUSSION

During obesity, pro-inflammatory macrophages accumulate in metabolic tissues, including AT [1,2], and contribute to obesity-associated IR both locally and systemically [11]. Since this novel discovery, much effort has been focused on determining mechanisms by which macrophages accumulate in obese AT. The overwhelming majority of these studies have sought to identify recruitment-dependent mechanisms for the increase in ATM number during obesity.

Much work has focused around the central hypothesis that obesity increases circulating inflammatory Ly6C^{hi} monocytes that are then recruited to AT via chemoattractants. Thus, recruitment-dependent mechanisms for increased ATMs should be contingent upon increased circulating inflammatory monocytes and chemotaxis of these cells to AT during HFD feeding. Despite the logical nature of this hypothesis, recent findings have called into question whether chemoattractant-mediated monocyte recruitment is the sole mechanism regulating ATM number during obesity. First, single gene deletion of multiple chemokines or chemokine receptors such as *Ccl3* [18], *Ccr5* [15], and *Cx3cr1* [17], does not modulate ATM number during HFD feeding. Even in studies demonstrating that a chemokine or its receptor plays a role in promoting macrophage accumulation in obese AT, ATM number is not normalized to levels observed in lean AT [21–23,48]. Second, in *Ccr2*−/− mice, there is a near absence of circulating Ly6C^{hi} cells [49], yet there is either no difference in ATM numbers or these differences are noted only after long periods of HFD feeding [13,21,48]. Third, MGL1 has been identified as a critical factor regulating the survival and migration of Ly6C^{hi} monocytes, as animals deficient in MGL1 do not mobilize Ly6C^{hi} monocytes from the bone marrow to the blood in response to HFD feeding [24]. However, despite

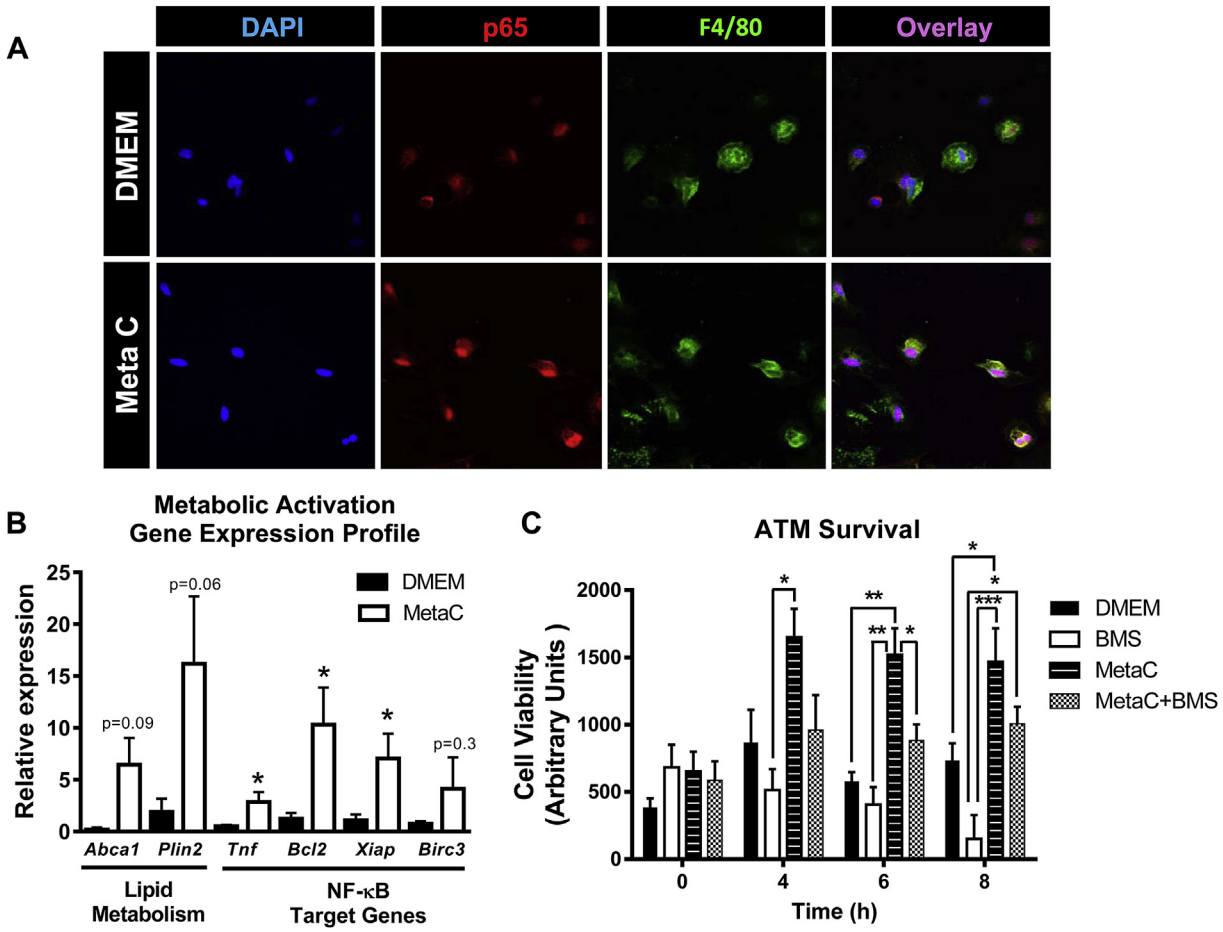

Figure 7: Inhibition of NF-κB activity decreases ATM survival in an obesogenic setting. Male C57Bl/6 mice were placed on a HFD for 3 weeks to obtain sufficient numbers of ATMs for *ex vivo* studies. A) Nuclear translocation of NF-κB. Adhesion-selected ATMs were treated with the metabolic cocktail (MetaC, 30 mM glucose, 10 nM insulin, 0.4 mM of palmitic acid) for 30 min and subsequently stained with DAPI (blue), p65 (red), and F4/80 (green). Magnification: 60× with a 1.5 zoom. B) Gene expression. ATMs were treated with the MetaC for 2 h and RNA isolated for real-time RT-PCR analysis of expression of lipid metabolism (*Abca1* and *Plin2*) as well as NF-κB-driven pro-inflammatory (*Tnf*) and pro-survival (*Bcl2*, *Xiap*, *Birc3*) genes. C) Cell viability. ATMs were treated with DMEM (control), MetaC, BMS-34551 (BMS), or MetaC + BMS for 0–8 h. Cell viability was detected using the Cell-Titer Blue assay as described in the Methods. Data are presented as mean ± SEM, n = 4–5/group. *p < 0.05, **p < 0.01, ***p < 0.001 between groups.

the near absence of circulating pro-inflammatory monocyte populations, deletion of *Mgl1* does not normalize ATM number to levels observed in lean AT [24]. This dissociation between the chemoattractant potential of AT, circulating blood monocyte number, and ATM content suggests that an increase in the recruitment of inflammatory Ly6C^{hi} monocytes is not the only mechanism regulating ATM accrual during obesity. Indeed, taken together, these published reports suggest that recruitment-independent mechanisms for macrophage accrual in obese AT should be considered.

Potential recruitment-independent mechanisms that could also play a role in the regulation of ATM number during obesity include: increased proliferation of macrophages within AT, decreased egress of macrophages from AT, or increased ATM survival. Recent studies now show that increased proliferation and decreased egress of ATMs can, in fact, contribute to ATM accumulation during obesity [25–27]. We now suggest that macrophage longevity is an additional metabolically regulated process that, when dysregulated during obesity, promotes macrophage survival and accumulation in AT, thus contributing to the diminished function of the tissue.

In agreement with this idea, recent studies show that macrophage apoptosis occurs infrequently in obese AT. For example, sophisticated imaging studies in AT explants demonstrate very few apoptotic macrophages in obese AT [50]. Furthermore, these studies showed that macrophages within the CLS of obese AT were stable, showing no shrinkage or cell death, over the 7-day imaging time-course, suggesting that ATMs in obese AT are long-lived [50]. In contrast, another study reported high levels of macrophage apoptosis in the AT of obese pregnant women [51]. However, these studies are difficult to interpret in the context of our results, as pregnancy is an extremely complex physiological state. Beyond this, there have also been hints in the literature that decreasing macrophage survival in AT of obese mice and humans reduces the metabolic abnormalities associated with obesity. Feng et al. showed that activation of ATM apoptosis via treatment with liposomal clodronate decreased AT inflammation and improved systemic glucose tolerance and insulin sensitivity in a mouse model of obesity [52]. Additionally, Kern and colleagues reported that pioglitazone, an insulin sensitizing TZD, increased macrophage apoptosis in human AT, possibly contributing to the reduced ATM number observed after TZD treatment [53,54]. These findings demonstrate that pharmacological activation of macrophage apoptosis in obese AT reduces ATM content and improves metabolic function. If ATM apoptosis can be manipulated to improve AT function, it is logical that macrophage

survival may also be regulated in a physiologically relevant manner to control macrophage content of AT.

Our studies showed that ~17% of ATMs were TUNEL$^+$ in the lean AT. This is quite surprising, given that one might expect efferocytic processes to quickly clear the apoptotic cells. However, this finding is in agreement with published literature. In their work using AT-specific p65 knockout mice (discussed in more detail below), Gao et al. also showed a fair amount of TUNEL staining in wild type lean AT [55]. Furthermore, studies by Cai et al. demonstrated significant macrophage apoptosis (22% of macrophages were TUNEL positive) and turnover (35% turnover rate in 48 h) in interstitial macrophages from the lung tissue of healthy rhesus macaques [56]. In agreement with these findings, tissue macrophages in murine lung were found to have substantial turnover during a 21-day study, and these macrophages were replaced through a self-renewal process [57]. Together, these studies support the idea that significant macrophage apoptosis/turnover occurs in multiple tissues of healthy animals. It should also be noted that about 10–20% of the TUNEL$^+$ were not macrophages. These cells could be adipocytes, as has been reported [41]; however, they could also include other immune cells such as neutrophils, T cells, B cells, or eosinophils. Further studies are needed to determine whether apoptosis of other leukocytes takes place in AT and whether this is of relevance to AT homeostasis.

In other metabolic settings, control of macrophage death/survival is known to be important for disease progression. For example, in atherosclerotic lesions, macrophage apoptosis and clearance by other efferocytic macrophages protects from early lesion formation [58,59]. Conversely, decreased macrophage apoptosis or impaired efferocytosis in advance lesions contributes to plaque instability [60]. Of potential relevance to ATMs, Tabas and colleagues have shown that prior engagement of Toll Like Receptor 4, *i.e.* activation of an acute inflammatory pathway, protects macrophages from subsequent apoptosis in settings of sustained ER stress [61]. This pathway is suggested to prolong cell survival to allow for continued production of inflammatory cytokines and antimicrobial proteins in order to remove the infectious insult. Because chronic activation of ATMs during obesity can activate similar inflammatory pathways, these cells may be "tricked" into survival, with the ultimate result being detrimental rather than protective. In fact, both our *in vivo* and *ex vivo* studies support the notion that activation of macrophages increases their survival. These data suggest that modulation of macrophage survival is beneficial in the setting of microbial infection, but that activation of these same pathways may be a significant contributor to the pathological processes occurring during obesity by promoting both the survival and the inflammatory nature of ATMs.

Inflammatory activation of macrophages is largely regulated by the transcription factor, NF-κB. Studies by Chiang et al. demonstrated increased nuclear translocation of the p65 subunit of NF-κB in ATMs from obese compared to lean mice [33], suggesting that ATM inflammation may be driven by NF-κB-dependent mechanisms. Although NF-κB is often appreciated for its pro-inflammatory role, this transcription factor also acts as a potent pro-survival factor. Our data demonstrate that the pro-survival axis of NF-κB is initiated in ATMs during obesity, as indicated by increased p65 nuclear localization, elevated NF-κB–driven luciferase activation, increased Bcl-2 protein levels and mitochondrial localization, and elevated expression of IAP genes. These data demonstrate that obesity-driven NF-κB activity not only promotes an inflammatory phenotype in ATMs in obese AT, but also increases the expression of pro-survival genes/proteins. Further, our *ex vivo* studies suggest that NF-κB activity is necessary for increase ATM survival under obesogenic conditions.

Our use of the inhibitor BMS-34551 to inhibit NF-κB specifically in ATMs is a novel model that has given great insight in to the contribution of this pathway to ATM survival. BMS-345541 has been previously demonstrated to be highly effective at inhibiting NF-κB transcriptional activity via its specificity to the NF-κB activator, IKK [47]. Importantly, the compound was tested against a panel of 15 other kinases, including c-Jun, STAT3, and MAPK, and failed to inhibit the activity of these inflammatory factors [47]. Furthermore, it has been demonstrated that treatment of NGL bone marrow derived macrophages with BMS-345541 significantly decreased LPS induced NF-κB transcriptional activity [34,47,62]. MetaC-mediated upregulation of NF-κB was also inhibited by BMS in our ATMs (Supplemental Figure 5B). Although this specificity has been shown in other cell types, we cannot rule out that there could be off-target effects on pathways other than NF-κB that control ATM apoptosis. Of note, this could alter the interpretation of our pharmacological data. In light of this, future studies, such as genetic manipulation of NF-κB in ATMs, should be performed to better identify the importance of this transcription factor in regulating ATM survival.

As this manuscript was in preparation, Gao et al. reported their findings regarding inflammation in an AT-specific p65 knockout model (driven by the ap2 promoter, *i.e.* deletion in adipocytes and likely macrophages) [55]. Surprisingly, absence of p65 resulted in different effects in lean versus obese mice. They demonstrated that absence of the p65 subunit of NF-κB reduced inflammation and ATM content in lean mice — presumably due to the absence of the inflammatory arm of NF-κB signaling in the lean setting. In contrast, absence of p65 in obese mice led to adipocyte apoptosis — indicating the absence of the survival arm of NF-κB in the obese setting. In addition, ATM numbers and overall AT inflammation were increased during obesity — most likely as a consequence of the adipocyte death. Importantly, the authors also noted that ATM apoptosis was elevated in the p65-null obese mice, a finding they attributed to the absence of p65-mediated pro-survival signaling in the ATMs [55]. These results suggest that adipocyte apoptosis and macrophage apoptosis may have different outcomes in regards to increasing or decreasing macrophage number in AT. The increased ATM content found in this model may be solely due to an immense and overwhelming amount of adipocyte cell death, which likely induced macrophage recruitment to AT. In this case, deletion of p65 in both the adipocytes and macrophages makes it complicated to determine the contribution of each process to the regulation of ATM number. However, these data further support our findings that NF-κB controls ATM apoptosis/survival.

Our studies demonstrate that increased markers of ATM survival in the obesogenic environment may be NF-κB-dependent. However, ATM survival may also be regulated by additional mechanisms. Kratz et al. demonstrates that ATMs in obese AT display a "metabolic activation" phenotype [39]. An aspect of this phenotype is the induction of sequestome-1 (p62). These authors suggested that uptake of palmitic acid induces not only NF-κB activation, but also results in impaired autophagy. Interestingly, several studies suggest a role for both autophagic degradation and NF-κB signaling pathways in regulating cell survival [63]. Interestingly, NF-κB activates pro-survival regulators, Bcl-2 and Bcl-xl, which inhibit key players in autophagy, including Beclin 1. The inhibition of autophagosome formation can lead to the accumulation of p62. Together, the above findings suggest that decreased autophagy in ATMs during obesity may be an additional mechanism contributing to increased cell survival. However, much of the literature suggests that the role of autophagy in inhibition or activation of cell survival is context dependent. Therefore, future research is needed to determine the role of autophagy in ATM survival.

An additional mechanism that may be involved in ATM survival is signaling through the nuclear factor E2-related factor-2 (Nrf2) pathway. Nrf2 is a transcription factor that is induced under oxidative stress conditions where it plays a role in inducing the transcription of anti-oxidant genes to counter the dangerous effects of reactive oxygen species. Like NF-κB, Nrf2 has been demonstrated to promote survival by inducing the transcription of pro-survival proteins Bcl-2 and Bcl-xl [64,65]. In regards to improving the ATM number and AT inflammatory state, global deficiency of Nrf2 protects against diet-induced obesity [66]. Furthermore, studies demonstrate that myeloid specific deletion of Nrf2 decreases the amount of CLSs in HFD fed mice; however, this deficiency does not protect from HFD-induced AT inflammation and insulin resistance [37]. Future studies are needed to better elucidate the role of Nrf2 in ATM number and AT inflammation during obesity as well as whether Nrf2 and NF-kB pathways intersect in ATMs.

Our data demonstrate that the obese AT micro-environment metabolically activates ATMs in a way that may promote their survival. Furthermore, NF-κB appears to be at the center of controlling this life and death balance. These findings, combined with recent literature demonstrating that increased proliferation and reduced egress of macrophages promote increased ATM content in obese AT, indicate that recruitment-independent mechanisms indeed also modulate ATM number during obesity. A further understanding of the relative contributions of recruitment, proliferation, egress, and survival to the control of ATM number and inflammatory status could pave the way for the development of novel therapeutics for the treatment of metabolic disorders.

ACKNOWLEDGMENTS

This project was supported by a Department of Veterans Affairs Merit Award (5I01BX002195) and by an American Heart Association Established Investigator Award (12EIA8270000) to AH Hasty. AA Hill was previously supported by the Cardiovascular Research Training Program (T32 HL007411-30) and is currently supported by an individual NRSA (F31DK100144). EK Anderson-Baucum was supported by AHA Pre-doctoral fellowship (12PRE11910047). Confocal imaging was performed in the Vanderbilt Cell Imaging Shared Resources Core through Vanderbilt University Medical Center's Digestive Disease Research Center supported by NIH grant P30DK058404 Core Scholarship. Image quantification experiments in Figures 5 and 6 were performed in the Vanderbilt High-throughput Screening Core Facility, which is an institutionally supported core, with assistance provided by Dehui Mi, Ph.D and Joshua Bauer, Ph.D. The authors have no financial interests to disclose. We would also like to thank the other members of the Hasty Laboratory, as well as Dario Gutierrez, for their comments and helpful suggestions on this manuscript.

CONFLICT OF INTEREST

None declared.

APPENDIX A. SUPPLEMENTARY DATA

Supplementary data related to this article can be found at http://dx.doi.org/10.1016/j.molmet.2015.07.005.

REFERENCES

[1] Weisberg, S.P., McCann, D., Desai, M., Rosenbaum, M., Leibel, R.L., Ferrante Jr., A.W., 2003. Obesity is associated with macrophage accumulation in adipose tissue. Journal of Clinical Investigation 112:1796–1808.

[2] Xu, H., Barnes, G.T., Yang, Q., Tan, G., Yang, D., Chou, C.J., et al., 2003. Chronic inflammation in fat plays a crucial role in the development of obesity-related insulin resistance. Journal of Clinical Investigation 112:1821–1830.

[3] Feuerer, M., Herrero, L., Cipolletta, D., Naaz, A., Wong, J., Nayer, A., et al., 2009. Lean, but not obese, fat is enriched for a unique population of regulatory T cells that affect metabolic parameters. Nature Medicine 15:930–939.

[4] Kintscher, U., Hartge, M., Hess, K., Foryst-Ludwig, A., Clemenz, M., Wabitsch, M., et al., 2008. T-lymphocyte infiltration in visceral adipose tissue: a primary event in adipose tissue inflammation and the development of obesity-mediated insulin resistance. Arteriosclerosis Thrombosis and Vascular Biology 28:1304–1310.

[5] Nishimura, S., Manabe, I., Nagasaki, M., Eto, K., Yamashita, H., Ohsugi, M., et al., 2009. CD8+ effector T cells contribute to macrophage recruitment and adipose tissue inflammation in obesity. Nature Medicine 15:914–920.

[6] Winer, S., Chan, Y., Paltser, G., Truong, D., Tsui, H., Bahrami, J., et al., 2009. Normalization of obesity-associated insulin resistance through immunotherapy. Nature Medicine 15:921–929.

[7] Winer, D.A., Winer, S., Shen, L., Wadia, P.P., Yantha, J., Paltser, G., et al., 2011. B cells promote insulin resistance through modulation of T cells and production of pathogenic IgG antibodies. Nature Medicine 17:610–617.

[8] Wu, D., Molofsky, A.B., Liang, H.E., Ricardo-Gonzalez, R.R., Jouihan, H.A., Bando, J.K., et al., 2011. Eosinophils sustain adipose alternatively activated macrophages associated with glucose homeostasis. Science 332:243–247.

[9] Elgazar-Carmon, V., Rudich, A., Hadad, N., Levy, R., 2008. Neutrophils transiently infiltrate intra-abdominal fat early in the course of high-fat feeding. Journal of Lipid Research 49:1894–1903.

[10] Choi, S.H., Hong, E.S., Lim, S., 2013. Clinical implications of adipocytokines and newly emerging metabolic factors with relation to insulin resistance and cardiovascular health. Front Endocrinol (Lausanne) 4:97.

[11] Olefsky, J.M., Glass, C.K., 2010. Macrophages, inflammation, and insulin resistance. Annual Review of Physiology 72:219–246.

[12] Huber, J., Kiefer, F.W., Zeyda, M., Ludvik, B., Silberhumer, G.R., Prager, G., et al., 2008. CC chemokine and CC chemokine receptor profiles in visceral and subcutaneous adipose tissue are altered in human obesity. The Journal of Clinical Endocrinology and Metabolism 93:3215–3221.

[13] Lumeng, C.N., DelProposto, J.B., Westcott, D.J., Saltiel, A.R., 2008. Phenotypic switching of adipose tissue macrophages with obesity is generated by spatiotemporal differences in macrophage subtypes. Diabetes 57:3239–3246.

[14] Inouye, K.E., Shi, H., Howard, J.K., Daly, C.H., Lord, G.M., Rollins, B.J., et al., 2007. Absence of CC chemokine ligand 2 does not limit obesity-associated infiltration of macrophages into adipose tissue. Diabetes 56:2242–2250.

[15] Kennedy, A., Webb, C.D., Hill, A.A., Gruen, M.L., Jackson, L.G., Hasty, A.H., 2013. Loss of CCR5 results in glucose intolerance in diet-induced obese mice. American Journal of Physiology. Endocrinology and Metabolism 305:E897–E906.

[16] Kirk, E.A., Sagawa, Z.K., McDonald, T.O., O'Brien, K.D., Heinecke, J.W., 2008. Monocyte chemoattractant protein deficiency fails to restrain macrophage infiltration into adipose tissue [corrected]. Diabetes 57:1254–1261.

[17] Morris, D.L., Oatmen, K.E., Wang, T., DelProposto, J.L., Lumeng, C.N., 2012. CX3CR1 deficiency does not influence trafficking of adipose tissue macrophages in mice with diet-induced obesity. Obesity 20:1189–1199.

[18] Surmi, B.K., Webb, C.D., Ristau, A.C., Hasty, A.H., 2010. Absence of macrophage inflammatory protein-1{alpha} does not impact macrophage accumulation in adipose tissue of diet-induced obese mice. American Journal of Physiology. Endocrinology and Metabolism 299:E437–E445.

[19] Kanda, H., Tateya, S., Tamori, Y., Kotani, K., Hiasa, K., Kitazawa, R., et al., 2006. MCP-1 contributes to macrophage infiltration into adipose tissue, insulin resistance, and hepatic steatosis in obesity. Journal of Clinical Investigation 116:1494–1505.

[20] Nara, N., Nakayama, Y., Okamoto, S., Tamura, H., Kiyono, M., Muraoka, M., et al., 2007. Disruption of CXC motif chemokine ligand-14 in mice ameliorates

obesity-induced insulin resistance. The Journal of Biological Chemistry 282: 30794–30803.
[21] Weisberg, S.P., Hunter, D., Huber, R., Lemieux, J., Slaymaker, S., Vaddi, K., et al., 2006. CCR2 modulates inflammatory and metabolic effects of high-fat feeding. Journal of Clinical Investigation 116:115–124.
[22] Tamura, Y., Sugimoto, M., Murayama, T., Ueda, Y., Kanamori, H., Ono, K., et al., 2008. Inhibition of CCR2 ameliorates insulin resistance and hepatic steatosis in db/db mice. Arteriosclerosis, Thrombosis, and Vascular Biology 28: 2195–2201.
[23] Ito, A., Suganami, T., Yamauchi, A., Degawa-Yamauchi, M., Tanaka, M., Kouyama, R., et al., 2008. Role of CC chemokine receptor 2 in bone marrow cells in the recruitment of macrophages into obese adipose tissue. The Journal of Biological Chemistry 283:35715–35723.
[24] Westcott, D.J., Delproposto, J.B., Geletka, L.M., Wang, T., Singer, K., Saltiel, A.R., et al., 2009. MGL1 promotes adipose tissue inflammation and insulin resistance by regulating 7/4hi monocytes in obesity. The Journal of Experimental Medicine 206:3143–3156.
[25] Amano, S.U., Cohen, J.L., Vangala, P., Tencerova, M., Nicoloro, S.M., Yawe, J.C., et al., 2014. Local proliferation of macrophages contributes to obesity-associated adipose tissue inflammation. Cell Metabolism 19:162–171.
[26] Haase, J., Weyer, U., Immig, K., Kloting, N., Bluher, M., Eilers, J., et al., 2014. Local proliferation of macrophages in adipose tissue during obesity-induced inflammation. Diabetologia 57:562–571.
[27] Ramkhelawon, B., Hennessy, E.J., Menager, M., Ray, T.D., Sheedy, F.J., Hutchison, S., et al., 2014. Netrin-1 promotes adipose tissue macrophage retention and insulin resistance in obesity. Nature Medicine 20:377–384.
[28] Curtin, J.F., Cotter, T.G., 2003. Apoptosis: historical perspectives. Essays in Biochemistry 39:1–10.
[29] Elmore, S., 2007. Apoptosis: a review of programmed cell death. Toxicologic Pathology 35:495–516.
[30] Youle, R.J., Strasser, A., 2008. The BCL-2 protein family: opposing activities that mediate cell death. Nature Reviews Molecular Cell Biology 9:47–59.
[31] Karin, M., 2009. NF-kappaB as a critical link between inflammation and cancer. Cold Spring Harbor Perspectives in Biology 1:a000141.
[32] Hoesel, B., Schmid, J.A., 2013. The complexity of NF-kappaB signaling in inflammation and cancer. Molecular Cancer 12:86.
[33] Chiang, S.H., Bazuine, M., Lumeng, C.N., Geletka, L.M., Mowers, J., White, N.M., et al., 2009. The protein kinase IKKepsilon regulates energy balance in obese mice. Cell 138:961–975.
[34] Everhart, M.B., Han, W., Sherrill, T.P., Arutiunov, M., Polosukhin, V.V., Burke, J.R., et al., 2006. Duration and intensity of NF-kappaB activity determine the severity of endotoxin-induced acute lung injury. Journal of Immunology 176:4995–5005.
[35] Pfaffl, M.W., 2001. A new mathematical model for relative quantification in real-time RT-PCR. Nucleic Acids Research 29:e45.
[36] Altintas, M.M., Rossetti, M.A., Nayer, B., Puig, A., Zagallo, P., Ortega, L.M., et al., 2011. Apoptosis, mastocytosis, and diminished adipocytokine gene expression accompany reduced epididymal fat mass in long-standing diet-induced obese mice. Lipids in Health and Disease 10:198.
[37] Meher, A.K., Sharma, P.R., Lira, V.A., Yamamoto, M., Kensler, T.W., Yan, Z., et al., 2012. Nrf2 deficiency in myeloid cells is not sufficient to protect mice from high-fat diet-induced adipose tissue inflammation and insulin resistance. Free Radical Biology & Medicine 52:1708–1715.
[38] Murano, I., Barbatelli, G., Parisani, V., Latini, C., Muzzonigro, G., Castellucci, M., et al., 2008. Dead adipocytes, detected as crown-like structures, are prevalent in visceral fat depots of genetically obese mice. Journal of Lipid Research 49:1562–1568.
[39] Kratz, M., Coats, B.R., Hisert, K.B., Hagman, D., Mutskov, V., Peris, E., et al., 2014. Metabolic dysfunction drives a mechanistically distinct proinflammatory phenotype in adipose tissue macrophages. Cell Metabolism 20:614–625.
[40] Grubbs, F., 1969. Procedures for detecting outlying observations in samples. Technometrics 11:1–21.
[41] Cinti, S., Mitchell, G., Barbatelli, G., Murano, I., Ceresi, E., Faloia, E., et al., 2005. Adipocyte death defines macrophage localization and function in adipose tissue of obese mice and humans. Journal of Lipid Research 46:2347–2355.
[42] Alkhouri, N., Gornicka, A., Berk, M.P., Thapaliya, S., Dixon, L.J., Kashyap, S., et al., 2010. Adipocyte apoptosis, a link between obesity, insulin resistance, and hepatic steatosis. The Journal of Biological Chemistry 285:3428–3438.
[43] Chipuk, J.E., Moldoveanu, T., Llambi, F., Parsons, M.J., Green, D.R., 2010. The BCL-2 family reunion. Molecular Cell 37:299–310.
[44] Lindsay, J., Esposti, M.D., Gilmore, A.P., 2011. Bcl-2 proteins and mitochondria–specificity in membrane targeting for death. Biochimica et Biophysica Acta 1813:532–539.
[45] Chen, C., Edelstein, L.C., Gelinas, C., 2000. The Rel/NF-kappaB family directly activates expression of the apoptosis inhibitor Bcl-x(L). Molecular Cell Biology 20:2687–2695.
[46] Gautier, E.L., Shay, T., Miller, J., Greter, M., Jakubzick, C., Ivanov, S., et al., 2012. Gene-expression profiles and transcriptional regulatory pathways that underlie the identity and diversity of mouse tissue macrophages. Nature Immunology 13:1118–1128.
[47] Burke, J.R., Pattoli, M.A., Gregor, K.R., Brassil, P.J., MacMaster, J.F., McIntyre, K.W., et al., 2003. BMS-345541 is a highly selective inhibitor of I kappa B kinase that binds at an allosteric site of the enzyme and blocks NF-kappa B-dependent transcription in mice. The Journal of Biological Chemistry 278:1450–1456.
[48] Gutierrez, D.A., Kennedy, A., Orr, J.S., Anderson, E.K., Webb, C.D., Gerrald, W.K., et al., 2011. Aberrant accumulation of undifferentiated myeloid cells in the adipose tissue of CCR2-deficient mice delays improvements in insulin sensitivity. Diabetes 60:2820–2829.
[49] Tsou, C.L., Peters, W., Si, Y., Slaymaker, S., Aslanian, A.M., Weisberg, S.P., et al., 2007. Critical roles for CCR2 and MCP-3 in monocyte mobilization from bone marrow and recruitment to inflammatory sites. Journal of Clinical Investigation 117:902–909.
[50] Gericke, M., Weyer, U., Braune, J., Bechmann, I., Eilers, J., 2015. A method for long-term live-imaging of tissue macrophages in adipose tissue explants. American Journal of Physiology, Endocrinology and Metabolism ajpendo 00075 02015.
[51] Haghiac, M., Vora, N.L., Basu, S., Johnson, K.L., Presley, L., Bianchi, D.W., et al., 2012. Increased death of adipose cells, a path to release cell-free DNA into systemic circulation of obese women. Obesity 20:2213–2219.
[52] Feng, B., Jiao, P., Nie, Y., Kim, T., Jun, D., van Rooijen, N., et al., 2011. Clodronate liposomes improve metabolic profile and reduce visceral adipose macrophage content in diet-induced obese mice. PloS One 6:e24358.
[53] Bodles, A.M., Varma, V., Yao-Borengasser, A., Phanavanh, B., Peterson, C.A., McGehee Jr., R.E., et al., 2006. Pioglitazone induces apoptosis of macrophages in human adipose tissue. Journal of Lipid Research 47:2080–2088.
[54] Di Gregorio, G.B., Yao-Borengasser, A., Rasouli, N., Varma, V., Lu, T., Miles, L.M., et al., 2005. Expression of CD68 and macrophage chemoattractant protein-1 genes in human adipose and muscle tissues: association with cytokine expression, insulin resistance, and reduction by pioglitazone. Diabetes 54:2305–2313.
[55] Gao, Z., Zhang, J., Henagan, T.M., Lee, J.H., Ye, X., Wang, H., et al., 2015. P65 inactivation in adipocytes and macrophages attenuates adipose inflammatory response in lean but not in obese mice. American Journal of Physiology. Endocrinology and metabolism 308:E496–E505.
[56] Cai, Y., Sugimoto, C., Arainga, M., Alvarez, X., Didier, E.S., Kuroda, M.J., 2014. In vivo characterization of alveolar and interstitial lung macrophages in rhesus macaques: implications for understanding lung disease in humans. Journal of Immunology 192:2821–2829.

[57] Hashimoto, D., Chow, A., Noizat, C., Teo, P., Beasley, M.B., Leboeuf, M., et al., 2013. Tissue-resident macrophages self-maintain locally throughout adult life with minimal contribution from circulating monocytes. Immunity 38:792–804.

[58] Arai, S., Shelton, J.M., Chen, M., Bradley, M.N., Castrillo, A., Bookout, A.L., et al., 2005. A role for the apoptosis inhibitory factor AIM/Spalpha/Api6 in atherosclerosis development. Cell Metabolism 1:201–213.

[59] Liu, J., Thewke, D.P., Su, Y.R., Linton, M.F., Fazio, S., Sinensky, M.S., 2005. Reduced macrophage apoptosis is associated with accelerated atherosclerosis in low-density lipoprotein receptor-null mice. Arteriosclerosis, Thrombosis, and Vascular Biology 25:174–179.

[60] Tabas, I., 2004. Apoptosis and plaque destabilization in atherosclerosis: the role of macrophage apoptosis induced by cholesterol. Cell Death and Differentiation 11(Suppl 1):S12–S16.

[61] Woo, C.W., Cui, D., Arellano, J., Dorweiler, B., Harding, H., Fitzgerald, K.A., et al., 2009. Adaptive suppression of the ATF4-CHOP branch of the unfolded protein response by toll-like receptor signalling. Nature Cell Biology 11:1473–1480.

[62] Yang, J., Amiri, K.I., Burke, J.R., Schmid, J.A., Richmond, A., 2006. BMS-345541 targets inhibitor of kappaB kinase and induces apoptosis in melanoma: involvement of nuclear factor kappaB and mitochondria pathways. Clinical Cancer Research 12:950–960.

[63] Scarlatti, F., Granata, R., Meijer, A.J., Codogno, P., 2009. Does autophagy have a license to kill mammalian cells? Cell Death Differentiation 16:12–20.

[64] Niture, S.K., Jaiswal, A.K., 2013. Nrf2-induced antiapoptotic Bcl-xL protein enhances cell survival and drug resistance. Free Radical Biology and Medicine 57:119–131.

[65] Niture, S.K., Jaiswal, A.K., 2012. Nrf2 protein up-regulates antiapoptotic protein Bcl-2 and prevents cellular apoptosis. The Journal of Biological Chemistry 287:9873–9886.

[66] Pi, J., Leung, L., Xue, P., Wang, W., Hou, Y., Liu, D., et al., 2010. Deficiency in the nuclear factor E2-related factor-2 transcription factor results in impaired adipogenesis and protects against diet-induced obesity. The Journal of Biological Chemistry 285:9292–9300.

